Atmos. Chem. Phys. Discuss., 9, 17265–17296, 2009
www.atmos-chem-phys-discuss.net/9/17265/2009/

Atmospheric Chemistry and Physics Discussions

This discussion paper is/has been under review for the journal *Atmospheric Chemistry and Physics (ACP)*. Please refer to the corresponding final paper in *ACP* if available.

Closing the Dimethyl Sulfide Budget in the Tropical Marine Boundary Layer during the Pacific Atmospheric Sulfur Experiment

S. A. Conley[1], I. Faloona[1], G. H. Miller[2], B. Blomquist[5], D. Lenschow[3], and A. Bandy[4]

[1]Department of Land, Air and Water Resources, University of California, Davis, CA, USA
[2]Department of Applied Science, University of California, Davis, CA, USA
[3]National Center for Atmospheric Research, Boulder, CO, USA
[4]Department of Chemistry, Drexel University, Philadelphia, PA, USA
[5]Department of Oceanography, University of Hawaii, Honolulu, HI, USA

Received: 3 July 2009 – Accepted: 4 August 2009 – Published: 14 August 2009

Correspondence to: S. A. Conley (saconley@ucdavis.edu)

Published by Copernicus Publications on behalf of the European Geosciences Union.

Abstract

Fourteen research flights were conducted with the National Center for Atmospheric Research (NCAR) C-130 near Christmas Island (2° N, 157° W) during the summer of 2007 as part of the Pacific Atmospheric Sulfur Experiment (PASE). In order to tightly constrain the scalar budget of DMS, fluxes were measured at various levels in the marine boundary layer (MBL) from near the surface (~30 m) to the top of the mixed layer (~500 m) providing greater accuracy of the flux divergence calculation in the DMS budget. The observed mean mole fraction of DMS in the MBL exhibited the well known diurnal cycle, ranging from ~50 pptv in the daytime to 110 pptv at night. Contributions from horizontal advection are included using a multivariate regression of all DMS flight data from within the MBL to estimate the mean gradients and trends. With this technique we consider the residual term in the DMS budget as an estimate of overall photochemical oxidation. Error analysis of the various terms in the DMS budget indicate that chemical losses acting on time scales of up to 110 h can be inferred with this technique. On average, photochemistry accounted for ~7.3 ppt hr^{-1} loss rate for the seven daytime flights, with an estimated error of 0.6 ppt/hr. The loss rate due to expected OH oxidation is sufficient to explain the net DMS destruction without invoking the action of additional oxidants (e.g. reactive halogens.) The observed ocean flux of DMS averaged 3.1 (±1.5) μmol m^{-2} d^{-1}, and generally decreased throughout the sunlit hours. The average entrainment flux at the top of the MBL was 2.5 μmol m^{-2} d^{-1}; therefore the flux divergence term in the budget equation only contributed an average increase of 1.3 ppt hr^{-1} to the mean MBL mole fraction. Over the entire mission, the horizontal advection contribution to the overall budget was 0.2 ppt hr^{-1}, indicating a mean atmospheric DMS gradient nearly perpendicular to the east-southeasterly trade winds and the chlorophyll gradient in the equatorial upwelling ocean. Nonetheless, horizontal advection was a significant term in the budget of any given flight, ranging from −1.5 to 2.3 ppt hr^{-1}, indicating a patchy and random seawater DMS distribution, and thus needs to be accounted for in budget studies.

1 Introduction

In 1987, the CLAW hypothesis, named for its authors (Charlson, Lovelock, Andreae and Warren)(Charlson et al., 1987) proposed one possible negative feedback mechanism by which living organisms (phytoplankton) could influence the temperature of the planet. Marine phytoplankton are the primary source of dimethyl sulfide (DMS) in the marine troposphere, and DMS is a major source of cloud condensation nuclei (CCN) in that same region (Pandis et al., 1994). The CLAW hypothesis proposes that phytoplankton productivity is likely to increase with a warming ocean resulting in a corresponding increase in surface water DMS concentration. The greater surface water DMS concentration would increase the flux of DMS from the ocean to the atmosphere which would lead to a further increase in the number of cloud condensation nuclei available, resulting in brighter, more persistent clouds. Ultimately, this process could affect the planetary albedo resulting in the reflection of more shortwave radiation out of the earth-atmosphere system, leading to a reduction in surface temperature. The Pacific Atmospheric Sulfur Experiment (PASE) was designed to investigate the flux of DMS from the ocean and the processing of gas and aerosol sulfur by the atmosphere in the remote marine boundary layer (MBL).

The atmospheric budget of DMS in the MBL is controlled by four principal processes: efflux from the ocean, vertical transport into the buffer layer (BuL) above the MBL, horizontal advection, and photochemical destruction. Following (Kowalski and Serrano-Ortiz, 2007), the mixing ratio budget can be written as:

$$\frac{\partial c}{\partial t} + \nabla(\cdot uc) = -L \tag{1}$$

where c is the DMS mixing ratio sum of the fluctuating component, c', and its ensemble mean value, u is the full turbulent wind field, and L represents the mean photochemical loss rate of DMS. (Turbulent fluctuations in the oxidant field are neglected here.) In this work, primed variables indicate departures from the mean and capitals or overbars indicate mean values. Several assumptions, listed below, are frequently made in order

to simplify budget calculations in the boundary layer.

1. The flow is incompressible; $\nabla \cdot u = 0$, where $u = (u, v, w)$.
2. The turbulence is horizontally homogeneous, implying that there is no horizontal variation in any of the mean turbulent quantities such as the horizontal turbulent fluxes , i.e. $\frac{\partial}{\partial x}(\overline{u'c'}) = 0$; $\frac{\partial}{\partial y}(\overline{v'c'}) = 0$

With these assumptions, we obtain a budget equation for the mean DMS mole fraction in the remote marine boundary:

$$\frac{\partial C}{\partial t} = -U\frac{\partial C}{\partial x} - V\frac{\partial C}{\partial y} - \frac{\partial}{\partial z}(\overline{w'c'}) - L \tag{2}$$

Fourteen research flights were conducted with the National Center for Atmospheric Research (NCAR) C-130 near Christmas Island (2° N, 157° W) during the summer of 2007 as part of the Pacific Atmospheric Sulfur Experiment (PASE). In order to tightly constrain the scalar budget of DMS, fluxes were measured at various levels in the marine boundary layer (MBL) from near the surface (∼30 m) to the top of the mixed layer(∼500 m) providing greater accuracy of the flux divergence calculation in the DMS budget. Traditionally, measurement of the surface flux and the flux at the top of the MBL have been challenging to obtain and previous researchers have resorted to parameterizations of these processes in attempts to close the budget (Nowak et al., 2001). PASE was a unique photochemical experiment in that the flight legs were structured such that each stack (approximately 3 per flight) included 30 min legs at four heights of interest: near the surface, the middle of the mixed layer, near the top of the MBL (z_i), and in the lower buffer layer. The buffer layer (BuL) is the intermittently turbulent, conditionally unstable region often containing trade wind cumuli that lies just above the MBL and below the trade wind inversion which was typically found at 1.5 km a.m.s.l. during PASE. Turbulent vertical fluxes were calculated from eddy covariance, i.e. Flux=$(\overline{w'c'})$, where w represents the vertical component of wind. During PASE, all of the terms in Eq. (2) but L were directly measured.

2 Boundary layer structure

During PASE, the mean MBL potential temperature (Θ) only varied between 296.5 K and 298.0 K, and the mean sea surface temperature (SST) between 298.4 K and 300.5 K. This results in nearly constant surface sensible and latent heat fluxes and an MBL with virtually no diurnal changes. Over the tropical oceans, a three-layer atmospheric structure typically exists with a turbulent MBL of roughly 500 m depth, overlain by an intermittently turbulent buffer layer (BuL) of approximately 1000 m depth, overlain by the free troposphere (FT). Separating the MBL from the BuL is a weak temperature inversion, while a much stronger trade wind inversion (TWI) separates the BuL from the FT. Most scalars within the MBL are well mixed, resulting in a mixing ratio profile that is nearly constant with altitude throughout the MBL. DMS rapidly falls off to near zero above the MBL top. This structure was previously documented during ACE1 (Russell et al., 1998). An example of this structure from research flight #3 (RF03) of PASE is shown in Fig. 1.

3 Methods

DMS was measured by a mass spectrometric method called atmospheric pressure ionization mass spectrometry using isotopically labeled standards (APIMS-ILS). This technique has been shown to be viable for calculating vertical fluxes via eddy covariance (Bandy et al., 2002; Faloona et al., 2005). The measurement has some attenuation at higher frequencies, but the amplitude was corrected using the expression obtained by Blomquist (2009). Initially, the intent was to fly 30 min Lagrangian circles, and drift with the mean MBL flow over time to minimize the contribution from horizontal advection. Difficulties arose with the circle patterns because the aircraft frequently passed through its own exhaust, which rapidly mixed vertically throughout the MBL. Therefore, the circles were abandoned and a chevron pattern consisting of two 15 min legs with a 60 degree turn in the middle was flown instead. The orientation of the legs was chosen

so that the mean wind bisected the angle of the chevron pattern. Unfortunately, this pattern resulted in substantial drift relative to the air mass being sampled. To correct for the non-Lagrangian sampling and the resultant drift of the DMS concentration over time (due to advection), a multi-variable linear regression was performed on all of the MBL data collected during each of the flights.

Previous measurements of DMS on Christmas Island (Bandy et al., 1996) demonstrated a consistent sinusoidal diurnal cycle in the concentration of DMS with a morning maximum around 4:30 a.m.(local) and an afternoon minimum around 4:30 p.m. The DMS concentration was thus assumed to be a function of the position, x, y, and z (all measured in meters) and time t (measured in hours), i.e. $C=f(x,y,z,t)$. Expanding f in a Taylor series about the spatial coordinates, including only the first order terms, and assuming the time dependence to be the combination of a diurnal sinusoid and a linear drift leads to:

$$C = \beta_0 + \beta_1 x + \beta_2 y + \beta_3 z + \beta_4 t + \beta_5 \cdot \sin(\frac{2\pi(t-\phi)}{24}) \quad (3)$$

The coefficients (β_1–β_5) represent the DMS derivatives in space and time. The phase term (ϕ) represents the time of day when the sinusoidal component of the variation crosses zero, around 10:30 a.m. The solution is then approached as a least squares problem using the 1-s data for both the DMS mole fraction as well as the position and time compiled from all portions of the flight below the inversion height, z_i.

Visually, the model reproduces the daily variation as shown in Fig. 2. For a quantitative measure of the fit, we calculated the coefficient of determination R^2 for each flight, defined as

$$R^2 = 1 - \frac{\sum (C_i - M_i)^2}{\sum (C_i - \overline{C})^2}, \quad (4)$$

where C_i are the actual values of the DMS mole fraction in the time series and M_i are the modeled values of the DMS mole fraction. The numerator is the sum of the

squares of the departures of the model prediction from the actual mole fraction, while the denominator is the variance in the observed DMS values. For the day flights, the average R^2 is 0.76 while for RF13 (night flight) it drops to 0.49. This apparent loss of fit quality is probably not indicative of a problem with the model, but simply a result of the diminished atmospheric variability during the night flights. Day and night, random instrumental noise remains the same while atmospheric variability is greatly reduced around the (~4 a.m. local time) diurnal maximum. Although RF06 and RF13 are labeled night flights, they were actually flown half before and half after sunrise to study the effects of twilight photochemistry.

The gradients in each of the horizontal directions (β_1, β_2) and the vertical (β_3) for the PASE flights are listed in Table 1. The horizontal gradient of DMS was fairly consistent, with all but one flight (RF14) indicating higher concentrations to the east, and every flight but RF08 showing higher concentrations to the north. Since the mean wind was typically from the southeast, the advection was a balance between negative advection by the meridional wind and positive advection by the zonal wind.

3.1 Flux divergence

In addition to the mean temporal and spatial changes the scalar budget equation includes two remaining terms: vertical flux divergence and photochemical loss. In principle, the contribution to the mean scalar budget from the flux divergence in Eq. (1) is $-\nabla\cdot(\overline{cu})$, where the overbar indicates Reynolds averaging. This deceivingly simple term is complicated by the fact that measurements of wind speeds include a significant component of atmospheric variability due to turbulence in the MBL. Breaking down the flux divergence into each of its components leads to:

$$-\nabla\cdot(\overline{cu}) = -\frac{\partial}{\partial x}(\overline{uc}) - \frac{\partial}{\partial y}(\overline{vc}) - \frac{\partial}{\partial z}(\overline{wc}) \tag{5}$$

Decomposing into mean and fluctuating components:

$$\nabla\cdot(\overline{cu}) = -\frac{\partial}{\partial x}(\overline{u}\cdot\overline{c}) - \frac{\partial}{\partial x}(\overline{u'c'}) - \frac{\partial}{\partial y}(\overline{v}\cdot\overline{c}) - \frac{\partial}{\partial y}(\overline{v'c'}) - \frac{\partial}{\partial z}(\overline{w}\cdot\overline{c}) - \frac{\partial}{\partial z}(\overline{w'c'}) \tag{6}$$

The contributions from horizontal turbulent fluxes were measured to be nearly two orders of magnitude smaller than the horizontal contribution by the mean wind. In the vertical, the flux is dominated by the turbulent component since $\overline{w}$ and $\partial w/\partial z$ are both small. Therefore, the mean term can be neglected:

$$\nabla\cdot(\overline{cu}) = -\frac{\partial}{\partial x}(\overline{u}\cdot\overline{c}) - \frac{\partial}{\partial y}(\overline{v}\cdot\overline{c}) - \frac{\partial}{\partial z}(\overline{w'c'}) \tag{7}$$

Using the incompressibility assumption, the first two terms in Eq. (7) can be converted from flux form to gradient form. With that in mind, the overall flux divergence is reduced to two components: horizontal advection by the mean wind and turbulent vertical mixing.

$$\nabla\cdot(\overline{cu}) = \overline{u}\frac{\partial\overline{c}}{\partial x} + \overline{v}\frac{\partial\overline{c}}{\partial y} + \frac{\partial(\overline{w'c'})}{\partial z} \tag{8}$$

Each of these terms is considered in detail in the next sections.

3.2 Horizontal advection

Figure 3 illustrates the evolution of the chlorophyll-a concentration in the ocean around Christmas Island during August 2007 in response to a developing weak La Niña. The SeaWiFS data shows that the concentration in the equatorial cold tongue increased substantially between the first and last week of August. Chlorophyll is frequently used as a weak proxy for DMS concentration (Simo and Dachs, 2002) and thus provides evidence that the region is horizontally inhomogeneous with respect to DMS production in the ocean. The PASE flights were typically within or near the equatorial cold tongue

and the variance in the horizontal is probably related to the varying levels of productivity indicated by this image. However, the persistent gradient in the in-situ data is directed to the north-northeast, and therefore appears to have a complex spatial relationship to the local chlorophyll patterns in the ocean.

The first two research flights consisted of Lagrangian circles while later flights used a chevron pattern. Each of these flight techniques resulted in differing levels of success tracking the mean wind. Table 1 shows the motion of the C-130 relative to the mean wind for each of the PASE research flights. Calculation of the horizontal advection budget term involves two steps: First, the zonal and meridional gradients in the DMS mole fraction are estimated using the multiple regression fit described above. Then, the mean wind is calculated by averaging each wind component measured during the legs flown within the boundary layer. The average wind direction during the PASE flights was from 105° while the average DMS gradient vector was oriented to the NNE (017°)–nearly perpendicular to the mean wind. Thus, on average, advection contributes nothing to the DMS budget. Nevertheless inclusion of this term was important for each flight because it contributed between 10–40% of the observed DMS rate of change.

3.3 Vertical flux divergence

The relatively insoluble DMS volatilizes from the sea surface to the lowest layers of the MBL, and is turbulently mixed throughout the MBL and carried to the BuL by convection. As can be seen in Fig. 1, its concentration drops rapidly with altitude above the MBL so very little DMS survives to enter the free troposphere. Flux divergence was estimated from the turbulent vertical flux (via eddy covariance) measured at various levels within the MBL. Figure 4 shows the co-spectra of DMS mole fraction and vertical wind speed grouped by approximate height above the surface and averaged over all of the PASE research flights. The labels correspond to the location within the MBL where the measurement was taken and roughly translate to the top and bottom of the MBL. As would be expected in the MBL, the cospectral peak is shifted to the left (lower wave numbers, larger eddies) as we move up in the MBL from the lower boundary layer

(LBL) to the top of the boundary layer (TBL).

A 200 s (22 km) averaging interval was selected by examining the complete co-spectra to find a frequency cut-off that would capture most of the flux without including mesoscale variations. As can be seen in Fig. 4, the contribution from wavenumbers below the cutoff (.045 km^{-1}) is small compared with wave numbers above the cutoff. This filter width is similar to but a little larger than that used during DYCOMS-II (Faloona et al., 2005). The longer filter width was chosen to capture all of the relevant scales evident in Fig. 4. The larger scales in PASE are possibly the result of convective roll structures that were often evident in cloud streets traversing the study area.

The vertical turbulent flux is determined using eddy covariance, or averaging the product of vertical wind perturbations and DMS mole fraction perturbations, i.e. ($\overline{w'c'}$) over each 22 km interval of a level flight leg. Since DMS and w are measured at different places on the airplane, and each instrument has its own characteristic delays, it is necessary to apply a time offset to synchronize the measurements. Since the DMS instrument has its own clock, this lag will vary from flight to flight and, in principle, could even drift from leg to leg within a given flight. The appropriate lag time was determined by examining the phase angle between DMS and w Fig. 5, with the assumption that the actual DMS and w are in phase. Since the DMS flux is usually largest for the LBL legs, those legs were used to determine the lag time for each flight stack. The average lag time for the PASE flights was ~1.4 s. Figure 6 shows the lag value determined for the same leg by maximizing the correlation coefficient instead. The difference of 1 sample (40 ms) makes a negligible difference in the flux.

In addition to correcting for the time lag, a correction must be made for the inability of the instrument to measure high-frequency variations. Laboratory testing with a fast switching valve at a known rate of change (0 and 3 hz) was used to estimate the signal attenuation through the full inlet with dryers relative to a short, straight inlet (Blomquist, 2009). From this laboratory study, a best fit equation for the attenuation of variance was determined to be:

$$\Phi^2(f) = \exp(-0.557 f^{0.917}). \quad (9)$$

The actual flux values (in frequency space) were divided by the square root of the above correction function to determine the corrected cospectra, which was then plotted versus wavenumber.

The final correction made to the flux involves correcting for temporal changes in the flux throughout the day. Because of a gradual decrease in the surface fluxes throughout each day, and because the difference between the BuL and MBL concentration changes throughout the day, the fluxes throughout the MBL decreased systematically during the course of each flight. Every stack (MBL, TBL, LBL) spanned nearly two hours and thus depending on the sequencing of the legs this temporal trend could lead to a significant error in the measured divergence. The fluxes were corrected by fitting a line to the flux versus time at each level and then correcting the fluxes measured for each stack to the center time of the stack. In practice this correction resulted in a small change to the divergence term in the budget (∼10%).

4 Results and discussion

The observed mean DMS mole fraction in the MBL exhibited the well known diurnal cycle, ranging from ∼50 pptv in the daytime to 110 pptv at night. Table 2 shows the budget of DMS during the PASE research flights. Some of the flights were not well suited for a budget analysis and were excluded from the table. Among those, RF04 was a cloud penetration flight over a much larger region than the other flights. RF07 and RF11 focused on the surface layer but lacked sufficient flux measurements through the rest of the MBL to allow a reasonable estimate of divergence. Problems with the airplane's inertial navigation system during RF09 and RF10 rendered the wind measurements unreliable, and problems with the DMS instrumentation excluded RF01. Each of the significant budget terms for the remaining MBL flights are listed in Table 2.

The columns in Table 2 relate to the terms in Eq. (2) and represent the bulk of the sources and sinks of DMS in the MBL.

From Table 2, the average photochemical loss rate during the day flights is

7.3 ppt hr^{-1}. Assuming the photochemical loss term is a first-order chemical reaction rate coefficient multiplied by the DMS mole fraction, the average loss rate for the daytime flights in Table 2 is 3.0×10^{-5} s^{-1}. This is considerably less than the maximum value of the unknown first-order loss rate estimated on the coast of Hawaii of 6.5×10^{-5} s^{-1} (De Bruyn et al., 2006).

It is assumed that the dominant chemical loss mechanism for DMS in the remote marine boundary layer is reaction with hydroxyl (OH). Because OH was in fact measured during most of the PASE flights, we can gain some confidence in the budget technique by comparing the expected loss to OH with the calculated photochemical term in the budget. During the daytime flights, the photochemical loss rate, inferred as the budget residual, averages 7.3 ppt hr^{-1}. Using the OH data from PASE (Mauldin, personal communication), with a daytime mean of 5×10^6 radicals/cm^3 and a maximum that varied between 6×10^6 radicals/$cm^3$to as much as 9×10^6 radicals/cm^3, and the DMS+OH rate constants from Sander et al. (2006), we estimate an average daytime loss of DMS to OH of 7.8 ppt hr^{-1}. During PEM-Tropics A, measurements of OH around Christmas Island had a daily maximum of around 8×10^6 radicals/cm^3 (Chen et al., 2001).

Another interesting observation that could prove useful to model parameterizations is the ratio of surface flux to BuL flux. On average, 80% of the DMS that enters the MBL from the sea surface is passed through to the overlying buffer layer. This is substantially higher than the 36% predicted in a modeling study by Lucas and Prinn (2002). In other words, the process of shallow convective pumping of DMS into the BuL and entrainment of low DMS air in the MBL passes most of the surface emission of DMS into the overlying BuL. The net entrainment velocities for the PASE flights are compiled in Table 2 with an average value of 1.7 cm/s during the day flights, and 2.2 cm/s for the night flights. During ACE1, the DMS-derived entrainment velocity varied from −4 cm/s to +4 cm/s (Russell et al., 1998). We should emphasize, however, that the entrainment velocities reported herein are dependent on the exact altitude of any particular BuL leg because of the large gradients in DMS that exist throughout the lower BuL (see Fig. 1). Comparisons to other values reported in the literature therefore need to be done with

considerable circumspection.

4.1 Cospectral similarity

In the surface layer, passive scalars are often assumed to exhibit a cospectral shape with w that is similar to that of Θ (Kaimal et al., 1972). Figure 10 shows the averaged, normalized cospectra for w with DMS, water vapor, and Θ for all of the flight legs below 50 m altitude during PASE. The universal Kaimal curve for neutral stability is shown in black and does indeed appear quite similar to Θ, but the peak and much of the covariance occur at higher wave numbers than the cospectra for the other two scalars. Previous investigators using Large Eddy Simulation (LES) also found significant differences in the cospectral shape of w with Θ and with passive scalars (Jonker et al., 1999). In their simulations it was observed that a principal driving factor in the cospectral distribution among low and high frequencies was the ratio of surface flux to entrainment flux. When the surface/entrainment flux ratio is around -0.5, the cospectral density is centered towards higher frequencies (similar to Θ and the universal Kaimal curve). However, when the surface/entrainment flux ratio approaches one, as is the case for water vapor and DMS over the ocean, the transport evolves to larger scales. This topic and detailed characterization of the MBL turbulence is covered in a subsequent manuscript (Conley et al., 2009.)

4.2 Flux profile evolution

In principle, the evolution of the vertical flux divergence term in the budget can be predicted through an examination of the difference between the DMS mixing ratio in the MBL and the BuL. Figure 9 shows the difference as a function of local time for all of the PASE flights. During the daylight hours, any pseudo-first-order photochemical loss is acting to reduce the DMS concentration in both the MBL and the BuL and, assuming similar OH concentrations in the two layers (Tan et al., 2001; Davis et al., 2001), each layer will experience the same loss, proportional to the DMS levels, thereby

reducing the absolute difference between the layers. Because the entrainment flux is proportional to the absolute concentration difference (assuming that the physical entrainment rate changes gradually over synoptic time scales and not diurnally) the net flux into the BuL will also decrease throughout the day.

The gas transfer velocity for DMS was determined as described by Blomquist et al. (2006), and then the bulk DMS seawater concentration was estimated for each stack by dividing the surface flux by the gas transfer velocity. These concentrations were then plotted as a function of time of day (Fig. 11). It appears that the concentration of DMS at the ocean surface does exhibit a diurnal trend during PASE, declining throughout the day. Although this is not commonly observed (Bailey et al., 2008), we conjecture that this might be due to solar warming of the ocean surface during the day increasing static stability of the ocean boundary layer, as well as direct photolysis and emission depleting dissolved DMS through the day. Advancing these ideas beyond conjecture, however, would require a careful budget from ship-based measurements to investigate the diurnal pattern in detail.

In any event, both the surface and entrainment fluxes appear to decrease throughout the daytime on average leading to no discernible daytime pattern in the vertical flux divergence term. Because the experimental conditions did not allow for measurements in the late evening, it is not known what happens to the flux divergence term during this period, but in a diel steady-state sense this term must compensate for daytime photochemical loss in the long run.

Nighttime flight operations were constrained by the absence of runway lights on Christmas Island. Therefore, flights were required to start late enough at night to ensure landing in full daylight. Consequently, the first MBL legs of the nocturnal flights occurred after 3:00 a.m.. As discussed in Sect. 3, the nighttime maximum occurred somewhere around 4:30 a.m., meaning that the night buildup of DMS was nearly complete by the time the aircraft arrived on station. At the time of the first leg on RF06, for instance, the concentration had already stabilized preventing an examination of the expected nighttime buildup. On RF13 the morning maximum did not occur until nearly

6:30 a.m. Fig. 7, half way through our second stack. Excluding the third stack, which took place in the early daylight, the observed rate of change was ∼3.5 ppt hr^{-1}. During that dark period, the vertical flux divergence averaged ∼3.4 ppt hr^{-1}. Assuming this flux divergence held throughout the 12 h of darkness, it would constitute an MBL source of ∼40 ppt/day. On average, the MBL DMS mole fraction was observed to decrease by ∼35 (±5) ppt during the daytime flights, thus we conclude that the flux divergence does indeed compensate for the photochemical destruction in the long term, but most of it occurs diametrically out of phase with destruction.

4.3 Error analysis

When the multiple regression model returns the solution for Eq. (3), each coefficient is returned along with the expected standard deviation of that coefficient. The net error in the budget table is calculated by adding together all of the errors in Eq. (3) in quadrature. That is, if the matrix **X** represents all of the predictor values in the time series i.e. x, y, z, t. Then the standard error of the i-th coefficient β_i is equal to M_{ii}, where $M = \sigma^2_{\mathrm{Err}}(\mathbf{X}'\mathbf{X})^{-1}$ and σ_{Err} represents the standard deviation of the residuals in the model. This technique was used to calculate the error in the advection and observed rate of change. The error in the flux divergence term was slightly different because the least squares minimization was performed on the 200 s flux averages, weighted by their standard deviations.

With the exception of RF11 which lacked sufficient flux measurements high in the MBL, the flights all have a net error of ∼0.7 ppt hr^{-1}. Dividing the average MBL DMS mole fraction of ∼71 ppt this error is equivalent to a time constant of ∼101 h. Therefore, in theory, any physical process that modifies the DMS concentration with a lifetime of ∼4 days or less can be detected by the scalar budget method executed in PASE.

4.4 Comparison to existing parameterizations

The direct measurements of DMS fluxes made during PASE provide an opportunity to compare the data to predictions of certain parameterizations used in biogeochemical models. For instance, Simo and Dachs (2002) suggest a DMS flux can be estimated from surface chlorophyll concentrations obtained by satellite. The authors suggest two regimes based on the ratio of Chlorophyll-*a* (Chl) to the oceanic mixed layer depth (MLD). Mixed layer depth was determined each flight day by examining the temperature profile from the nearest TAO buoy (2N,155W), which was within 50 km of the mean position of all the flights. The mixed layer depth increased slightly during the four week mission from ∼80 m on 10 August to 100 m on 2 September. From Fig. 3, the maximum Chl was ∼0.4 mg/m^3, equivalent to a maximum value for Chl/MLD of ∼0.005 mg/m^4, well below the regime where Chl needs to be considered in predicting the surface DMS concentration.

In this low Chl environment, the surface water DMS concentration predicted by Simo and Dachs (2002): $[\mathrm{DMS}]_{\mathrm{aq}} = \ln(\mathrm{MLD}) + 5.7$ which ranges from 1.1 nM to 1.3 nM.

We then estimate the flux of DMS from the sea surface with the parameterization (Blomquist et al., 2006):

$$F = [\mathrm{DMS}]_{\mathrm{aq}} \cdot k_w \tag{10}$$

Here, k_w is the gas transfer velocity for DMS. For conditions typical of PASE, (SST=27°C, U_{10}=8 m/s), k_w∼13 cm/hr. The estimated flux of DMS would be between 3.1 and 4.0 μmol m^{-2} d^{-1}, which is slightly more than the averaged measured surface flux during PASE of 3.0 μmol m^{-2} d^{-1}.

The average surface flux of ∼3.0 μmol/m^2-day observed during PASE is similar to that measured during 2003 in the eastern equatorial pacific ∼3±2 μmol/m^2-day (Huebert et al., 2004), and on the coast of Hawaii ∼3 μmol/m^2-day (De Bruyn et al., 2006).

5 Conclusions

DMS mole fraction and flux were measured in the remote MBL near Christmas Island (2N, 157W) during the summer of 2007. The expected diurnal pattern of early morning maximum, followed by decay throughout the day to a late afternoon minimum was observed. The mean daytime DMS mole fraction was ∼66 ppt, while the mean nighttime concentration was ∼100 ppt. The dynamical terms in the daytime DMS budget (vertical flux divergence and horizontal advection) were measured and found to contribute 1.3 ppt hr^{-1} and 0.2 ppt hr^{-1} respectively. The average day time loss rate was ∼5.8 ppt hr^{-1} leaving an average photochemical loss of ∼7.3 ppt hr^{-1}. The cospectral behavior of DMS vs. w was very similar to that of water vs. w but considerably different from potential temperature vs. w, which followed the Kaimal et al. (1972) model of cospectra in the surface layer. Using the surface fluxes to estimate the DMS concentration in the surface water, we found a diurnal cycle in DMS seawater concentration. Further research is required to confirm and understand this cycle as well as the cospectral behavior of DMS vs. w.

Acknowledgements. Ocean color data used in this study were produced by the SeaWiFS Project at Goddard Space Flight Center. The data were obtained from the Goddard Earth Sciences Distributed Active Archive Center under the auspices of the National Aeronautics and Space Administration. Use of this data is in accord with the SeaWiFS Research Data Use Terms and Conditions Agreement. Aircraft navigation data and atmospheric state variables provided by NCAR/EOL under sponsorship of the National Science Foundation (http://data.eol.ucar.edu). Hydroxyl data provided by R. L. Mauldin. Mixed layer depth calculated with temperature profiles from TAO buoys, TAO Project Office of NOAA/PMEL.

The National Center for Atmospheric Research is sponsored by the National Science Foundation. This work was made possible through a grant from the Atmospheric Chemistry Program of the National Science foundation (ATM-0627227).

References

Bandy, A. R., Thornton, D. C., Tu, F. H., Blomquist, B. W., Nadler, W., Mitchell, G. M., and Lenschow, D. H.: Determination of the vertical flux of dimethyl sulfide by eddy correlation and atmospheric pressure ionization mass spectrometry (apims), J. Geophys. Res.-Atmos., 107, 4743, doi:10.1029/2002jd002472, 2002.

Blomquist, B. H. B. and Fairall, C. W.: Determining the sea-air flux of dimethylsulfide by eddy correlation using mass spectrometry, Unpublished Manuscript, 2009.

Blomquist, B. W., Fairall, C. W., Huebert, B. J., Kieber, D. J., and Westby, G. R.: Dms sea-air transfer velocity: Direct measurements by eddy covariance and parameterization based on the noaa/coare gas transfer model, Geophys. Res. Lett., 33, L07601, doi:10.1029/2006gl025735, 2006.

Charlson, R. J., Lovelock, J. E., Andreae, M. O., and Warren, S. G.: Oceanic phytoplankton, atmospheric sulfur, cloud albedo and climate, Nature, 326, 655–661, 1987.

Chen, G., Davis, D., Crawford, J., Heikes, B., O'Sullivan, D., Lee, M., Eisele, F., Mauldin, L., Tanner, D., Collins, J., Barrick, J., Anderson, B., Blake, D., Bradshaw, J., Sandholm, S., Carroll, M., Albercook, G., and Clarke, A.: An assessment of hox chemistry in the tropical pacific boundary layer: Comparison of model simulations with observations recorded during pem tropics a, J. Atmos. Chem., 38, 317–344, 2001.

Davis, D., Grodzinsky, G., Chen, G., Crawford, J., Eisele, F., Mauldin, L., Tanner, D., Cantrell, C., Brune, W., Tan, D., Faloona, I., Ridley, B., Montzka, D., Walega, J., Grahek, F., Sandholm, S., Sachse, G., Vay, S., Anderson, B., Avery, M., Heikes, B., Snow, J., O'Sullivan, D., Shetter, R., Lefer, B., Blake, D., Blake, N., Carroll, M., and Wang, Y.: Marine latitude/altitude oh distributions: Comparison of pacific ocean observations with models, J. Geophys. Res.-Atmos, 106, 32691–32707, 2001.

De Bruyn, W. J., Dahl, E., and Saltzman, E. S.: Dms and so2 measurernents in the tropical marine boundary layer, J. Atmos. Chem., 53, 145–154, doi:10.1007/s10874-005-9000-z, 2006.

Faloona, I., Lenschow, D. H., Campos, T., Stevens, B., van Zanten, M., Blomquist, B., Thornton, D., Bandy, A., and Gerber, H.: Observations of entrainment in eastern pacific marine stratocumulus using three conserved scalars, J. Atmos. Sci., 62, 3268–3285, 2005.

Jonker, H. J. J., Duynkerke, P. G., and Cuijpers, J. W. M.: Mesoscale fluctuations in scalars generated by boundary layer convection, J. Atmos. Sci., 56, 801–808, 1999.

Kaimal, J. C., Izumi, Y., Wyngaard, J. C., and Cote, R.: Spectral characteristics of surface-layer turbulence, Q. J. Roy. Meteor. Soc., 98, 563–589, 1972.

Kowalski, A. S. and Serrano-Ortiz, P.: On the relationship between the eddy covariance, the turbulent flux, and surface exchange for a trace gas such as co2, Bound.-Lay. Meteorol, 124, 129–141, doi:10.1007/s10546-007-9171-z, 2007.

Lucas, D. D. and Prinn, R. G.: Mechanistic studies of dimethylsulfide oxidation products using an observationally constrained model, J. Geophys. Res.-Atmos., 107(26), 4201, ACH12–1–26, doi:10.1029/2001jd000843, 2002.

Nowak, J. B., Davis, D. D., Chen, G., Eisele, F. L., Mauldin, R. L., Tanner, D. J., Cantrell, C., Kosciuch, E., Bandy, A., Thornton, D., and Clarke, A.: Airborne observations of dmso, dms, and oh at marine tropical latitudes, Geophys. Res. Lett., 28, 2201–2204, 2001.

Pandis, S. N., Russell, L. M., and Seinfeld, J. H.: The relationship between dms flux and ccn concentration in remote marine regions, J. Geophys. Res.-Atmos., 99, 16945–16957, 1994.

Russell, L. M., Lenschow, D. H., Laursen, K. K., Krummel, P. B., Siems, S. T., Bandy, A. R., Thornton, D. C., and Bates, T. S.: Bidirectional mixing in an ace 1 marine boundary layer overlain by a second turbulent layer, J. Geophys. Res.-Atmos., 103, 16411–16432, 1998.

Sander, S. E. A.: Chemical kinetics and photochemical data for use in atmospheric studies, JPL Publication, 06, 26, 2006.

Simo, R. and Dachs, J.: Global ocean emission of dimethylsulfide predicted from biogeophysical data, Global Biogeochem. Cy., 16(4), p. 1078, doi:10.1029/2001gb001829, 2002.

Tan, D., Faloona, I., Simpas, J. B., Brune, W., Olson, J., Crawford, J., Avery, M., Sachse, G., Vay, S., Sandholm, S., Guan, H. W., Vaughn, T., Mastromarino, J., Heikes, B., Snow, J., Podolske, J., and Singh, H.: Oh and ho2 in the tropical pacific: Results from pem-tropics b, J. Geophys. Res.-Atmos., 106, 32667–32681, 2001.

Table 1. Terms in the advection calculation. Columns as follows: flight number, horizontal advection (ppt hr^{-1}), zonal DMS gradient (ppt deg^{-1}), meridional DMS gradient (ppt deg^{-1}), vertical DMS gradient (ppt km^{-1}), mean zonal wind (km hr^{-1}). U_a and V_a represent the mean drift velocity of the airplane (km hr^{-1}).

RF	Adv	$\partial_x C$	$\partial_y C$	$\partial_z C$	U	U_a	V	V_a
2	0.5	3.43	13.02	−15	−26	−11.3	2.8	1.2
3	−0.8	1.61	9.32	−19	−23	3.8	14.0	−0.5
5	2.1	5.90	8.46	6	−36	−1.4	−1.5	2.8
8	−0.5	0.36	7.02	−11	−24	−2.2	9.9	4.4
11	2.3	5.94	−8.45	−13	−28	−17.6	10.3	5.3
12	−1.1	6.27	22.00	−8	−26	−13.8	13.1	2.7
14	−1.2	−0.46	27.63	−27	−36	−10.0	4.2	0.6
Average	**0.2**	**3.29**	**11.29**	**−12**	**−29**	**−7.5**	**7.6**	**2.4**
6	1.5	5.43	3.12	−12	−31	−1.9	1.0	1.5
13	−0.5	3.85	14.16	−52	−38	0.5	15.6	3.5
Average	**0.5**	**4.64**	**8.64**	**−32**	**−34**	**−0.7**	**8.3**	**2.5**

Table 2. DMS budget terms for the flights that they could be measured. Columns are defined from left to right as follows: Observed rate of change, vertical flux divergence, horizontal advection, photo-chemical loss required to balance budget L in Eq. (2), all in units of ppt hr^{-1}. Net error is an estimate of the error in the photochemical term (ppt hr^{-1}). The remaining columns are entrainment velocity (cm s^{-1}), mean MBL DMS concentration (ppt), surface flux and flux into the overlying buffer layer (umol m^{-2} d^{-1}).

RF	Obs	Div	Adv	Chem	NetError	V_e	[DMS]ppt	SurfFlux	BuLFlux
2	−5.2	0.4	0.5	−6.1	0.4	1.4	49.7	1.8	1.7
3	−6.0	1.9	−0.9	−7.1	0.4	1.0	66.8	2.3	1.5
5	−4.7	4.1	2.1	−10.9	0.7	1.4	69.0	3.6	2.0
8	−5.6	0.8	−0.5	−5.8	0.4	1.7	56.2	2.8	2.4
11	−5.8	1.1	2.3	−9.2	1.4		74.5	2.9	2.7
12	−5.9	1.5	−1.1	−6.3	0.5	3.5	52.5	2.7	1.8
14	−7.7	−1.0	−1.2	−5.4	0.5	1.1	94.1	1.8	2.5
Avg	**−5.8**	**1.3**	**0.2**	**−7.3**	**0.6**	**1.7**	**66.1**	**2.6**	**2.1**
6	0.6	−0.9	1.4	0.0	0.7	1.8	87.3	2.7	3.1
13	3.7	3.0	−0.5	1.2	0.7	2.6	112.9	6.8	4.8
Avg	**2.2**	**1.1**	**0.5**	**0.6**	**0.7**	**2.2**	**100.1**	**4.8**	**3.9**

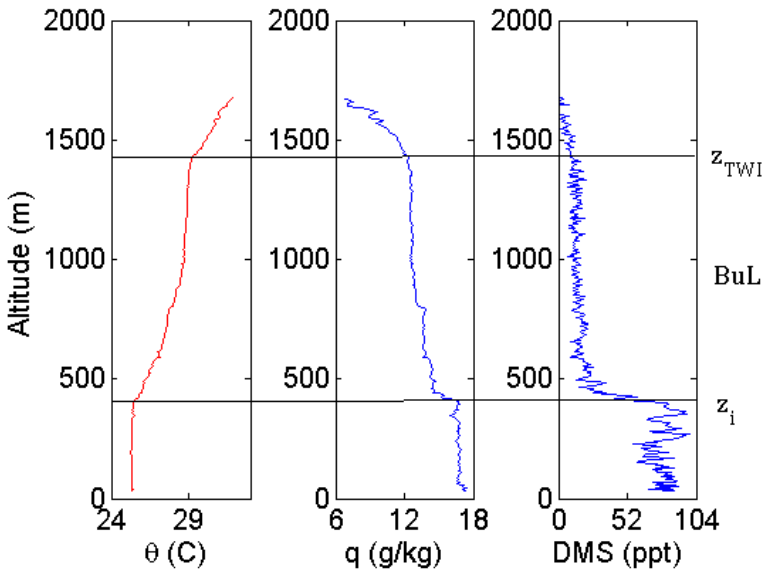

Fig. 1. RF02 MBL Structure Observed During PASE. z_i is the mean height of the weak MBL inversion and z_{TWI} denotes the stronger trade wind inversion aloft. Horizontal axes are potential temperature, water vapor, and DMS respectively.

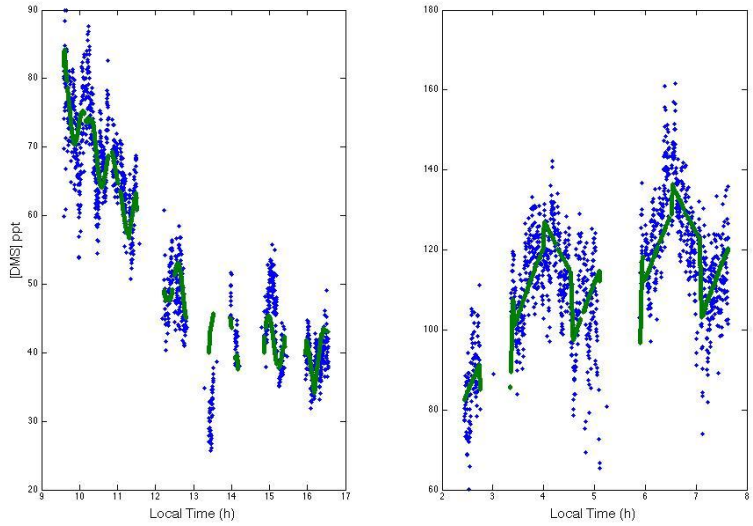

Fig. 2. Model fit of the time series of DMS observed in the marine boundary layer during RF02 (left, daytime) and RF13 (right, nighttime). Actual data points in blue, model fit in green.

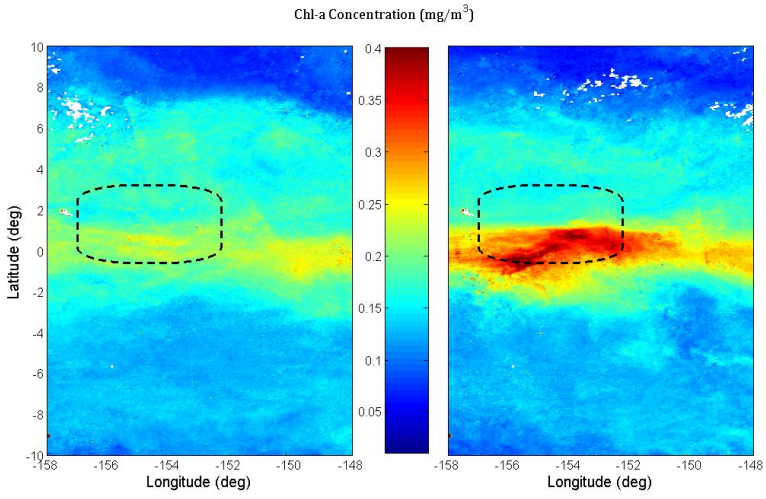

Fig. 3. PASE research flight area (dashed rectangle) in relation to the regional chlorophyll-a patterns for August 2007. The panel on the left is a composite of the first two weeks of August and the panel on the right is the last two weeks of August. The prevailing MBL winds during PASE were east-southeasterly with an average speed of 8 m/s.

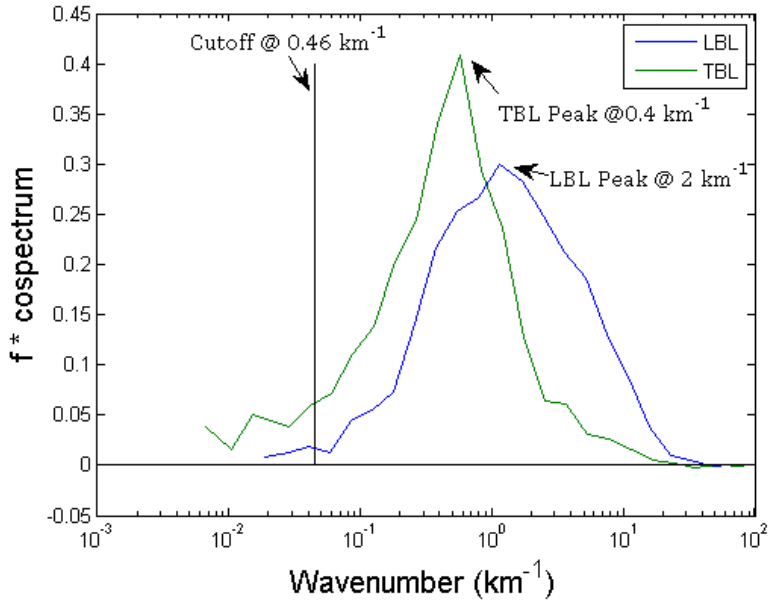

Fig. 4. Averaged co-spectra of DMS with vertical wind speed. The flight legs are averaged into lower levels (LBL) flown below 50 m, top of the boundary layer (TBL) flown around 400 m.

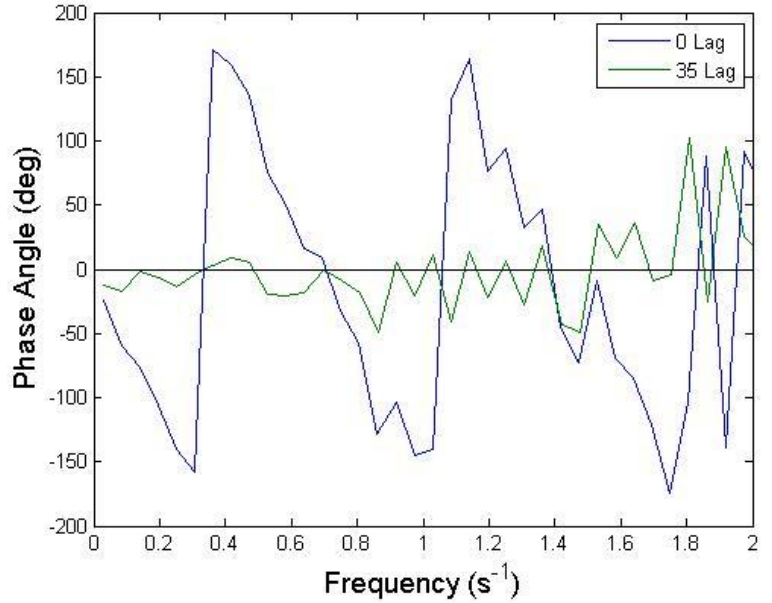

Fig. 5. Phase angle spectrum of DMS vs. *w* for leg 7 of RF03. Following the blue line, the difference between the first two zero crossings is 0.72 hz, which equates to 1.4 s, or 35 samples (at the high rate sampling of 25 hz). The green line shows the phase lag when the DMS signal is consequently shifted by 35 samples.

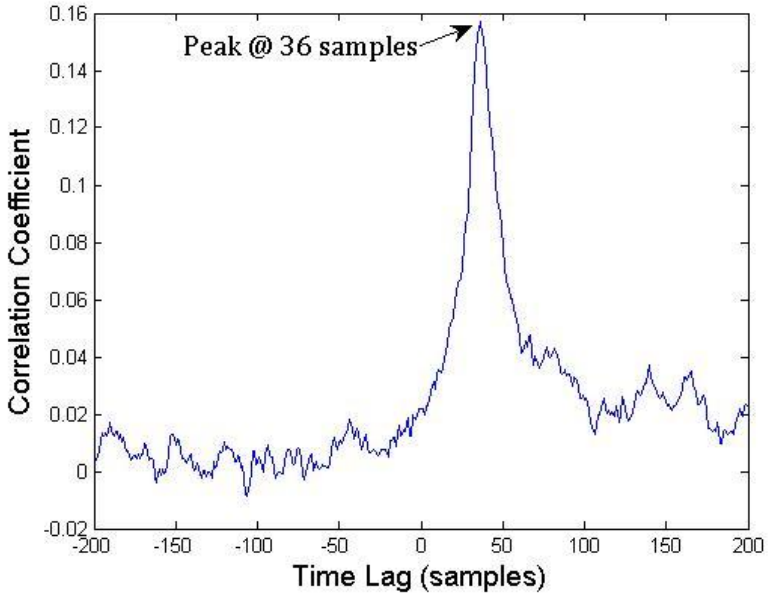

Fig. 6. Correlation coefficient between DMS and vertical wind as a function of time lag for leg 7 (LBL1.1) of RF03. The maximum correlation at (36/25=) 1.44 s is consistent with the lag time derived from the phase angle spectrum.

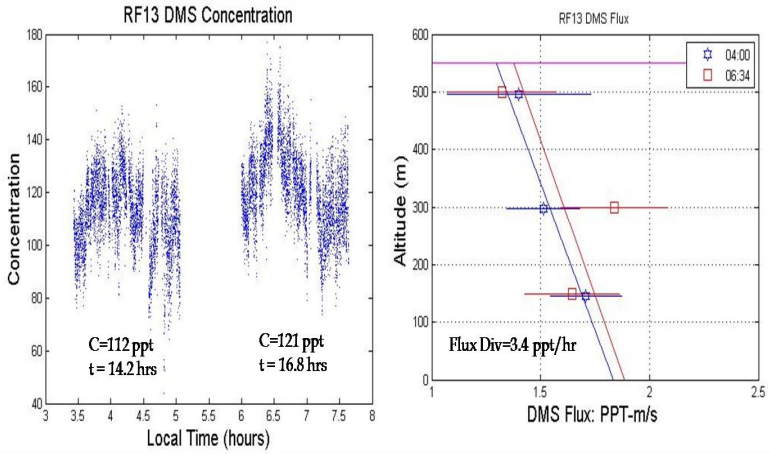

Fig. 7. RF13 DMS concentration (left) and flux profile (right). Between stacks 1 and 2, the concentration increased by 9 ppt over 2.6 hrs, or 3.5 ppt hr^{-1}. The right plot shows the flux profile observed on the two predawn stacks (blue stars – between 0300-0500, red squares – between 0530-0730) which indicates an average flux convergence of 3.4 ppt hr^{-1}.

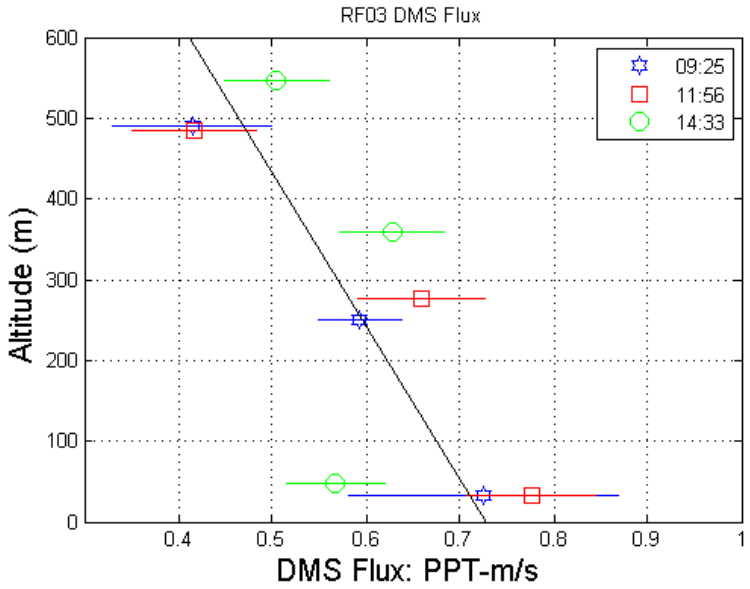

Fig. 8. DMS flux profile for RF03. The colors (red, blue and green) correspond to the three stacks of MBL legs flown in the morning, afternoon and late afternoon.

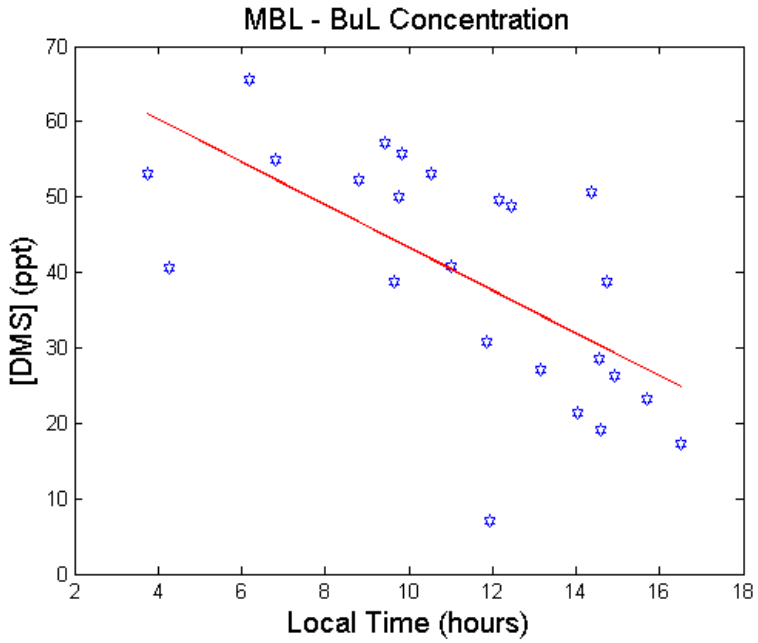

Fig. 9. Difference in DMS concentration between MBL and BuL for all PASE flights by time of day. R^2=0.42. On average, mean concentration difference decreased at a rate of = 2.8 ppt hr^{-1}.

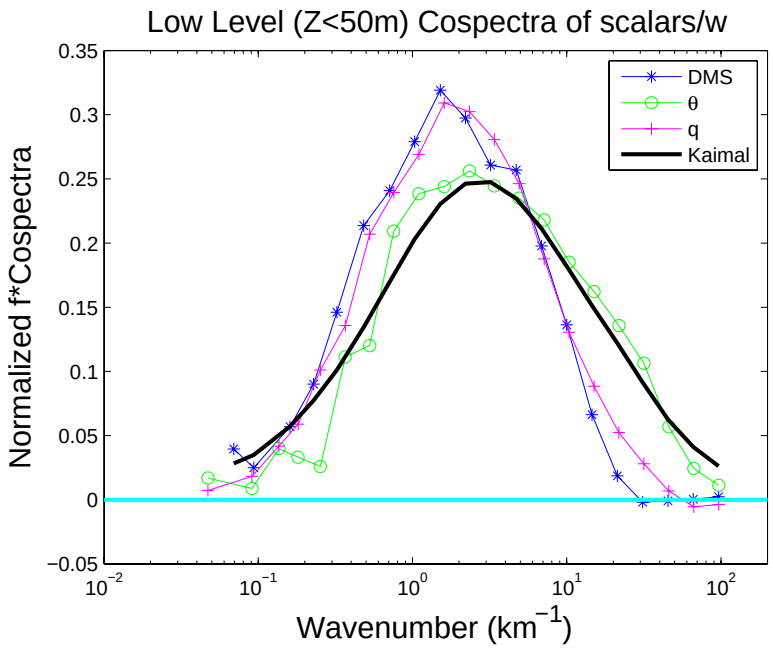

Fig. 10. Averaged Co-Spectra between DMS, θ, specific humidity (q), and vertical wind speed for the low level (z<50 m) legs for all of the PASE flights.

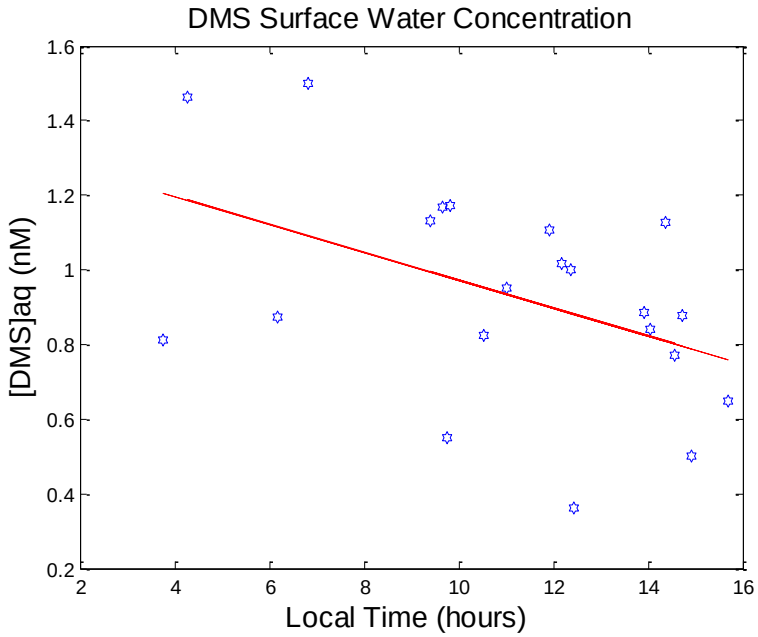

Fig. 11. Surface water DMS concentration estimated from the observed bulk parameterization of Blomquist et al. (2006) for all of the PASE flights as a function of time of day. R^2 for this plot is 0.22 and the slope is –.03 nM hr-1.